Supporting Information

Regulating the thickness of nanofiltration membrane for efficient water purification

Ke Tang[a,#], LinSheng Zhu[a,#], Piao Lan[a], YunQiang Chen[b], Zhou Chen[a,*], Yihong Lan[b], WeiGuang Lan[a,b,*]

[a] Mr. K. Tang, Mr. L.S. Zhu, Mr. P, Lan, Dr. Z. Chen, Prof. W.G. Lan
Xiamen University Center for Membrane Application and Advancement, College of Materials, Xiamen University, Xiamen 361005, Fujian, China.

[b] Dr. Y.H. Lan, Mr. Y.Q. Chen
Suntar Membrane Technology (Xiamen) Co., Ltd., Xiamen 361022, Fujian, China.

# These authors contributed equally to this work.

Corresponding authors: Dr. Z. Chen (zhouchen@xmu.edu.cn); Prof. W.G. Lan (wglan@xmu.edu.cn)

1 Experimental

1.1 Membrane characterization

The surface and cross-section morphology of various composite membranes were studied by a Field emission scanning electron microscopy (FE-SEM, Hitachi SU-70, Japan). The surface morphology and the element distribution of GO and GP complex were studied by a transmission electron microscopy (TEM, JEOL JEM-F200, Japan). Fourier transform infrared spectroscopy (FTIR, Nicolet 6700, USA) was analyzed over the range of 500-3000 cm^{-1}. The surface elemental composition of the GO and GP composite membranes was examined *via* the X-ray photoelectron spectroscopy (XPS, Thermo Scientific ESCALAB Xi+, USA). The X-ray source was Al-Kα radiation and the binding energies were referred to the C 1s peak (284.8 eV). Atomic force microscopy (AFM, Keysight MI5500, USA) was used to measure the membrane morphology and surface roughness. Ultraviolet-visible spectroscopy (UV-vis, Persee Co, TU-1901) was detected to the absorbance of PIP in n-heptane. In addition, water contact angles were tested *via* a contact angle tester (DSA100, KRUSS, Germany).

1.2 Computational simulations

The molecular structures used in this simulation were modeled using the software Gromacs 2019.6.[1] And molecular dynamics (MD) simulations were performed using the same software. TIP3P model, GAFF force field was used for MD simulations, and the effect of the GP complex on PIP diffusivity during interfacial polymerization was investigated. In the hexane–water system, there were 228 PIP molecules and 18000 water molecules in the aqueous phase, while in the organic phase there were 10 TMC and 1540 hexane molecules. In the hexane–water-GP system, one GO molecule and 18 PhA molecules were further added into the aqueous phase. TIP3P model was used for water,[2] while GAFF force field[3] was adopted for all other species. Lennard-Jones potential was used for van der Waals interactions. Electrostatic interactions were computed with particle-mesh Ewald method. Energy minimization was performed to relax the initial conformation. Then, 20-ns production runs with a time step of 2 fs were performed at 298.15 K and 1 bar, with V-rescale thermostat and Berendsen barostat.

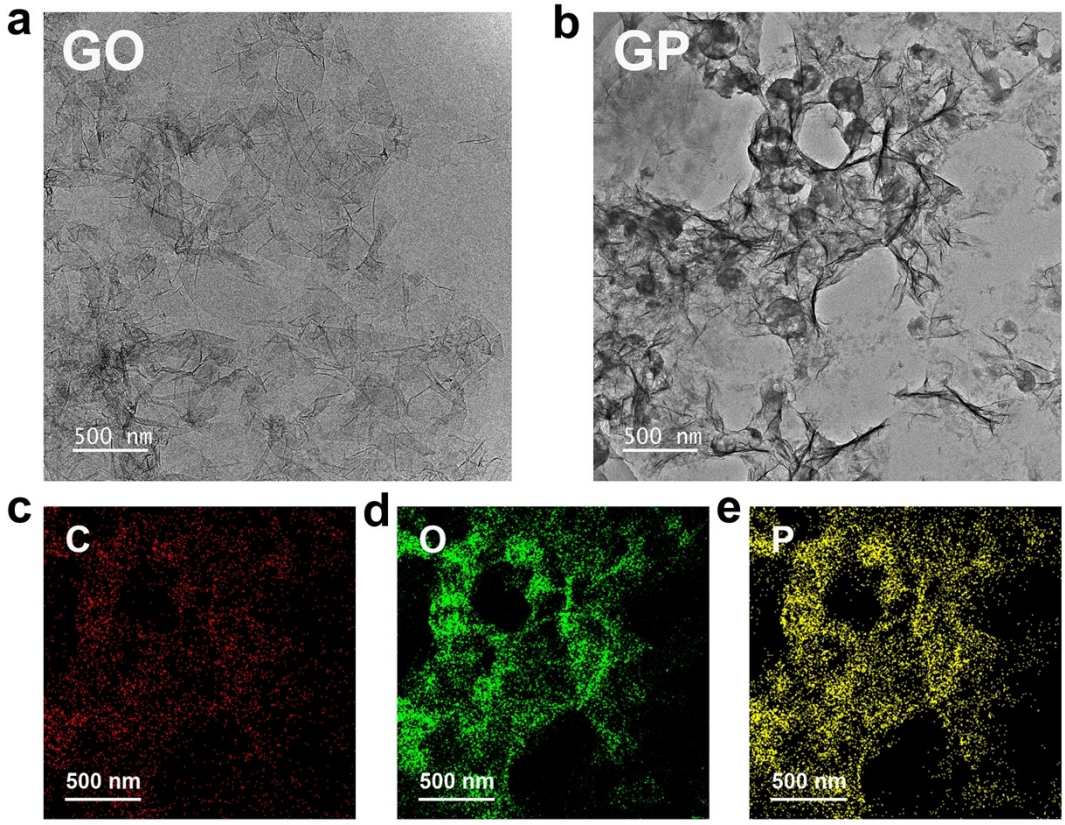

Figure S1. TEM images of (a) GO and (b) GP complex. Corresponding elemental mapping of (c) C, (d) O, (e) P.

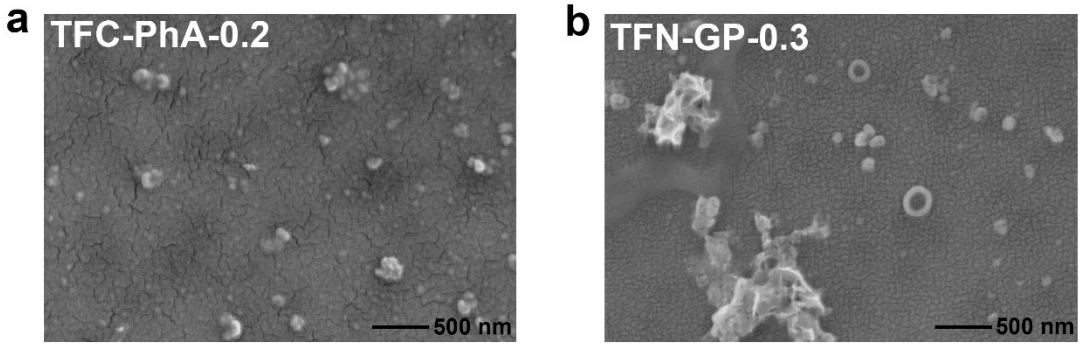

Figure S2. SEM surface images of (a) TFC-PhA-0.2 and (b) TFN-GP-0.3 composite membranes.

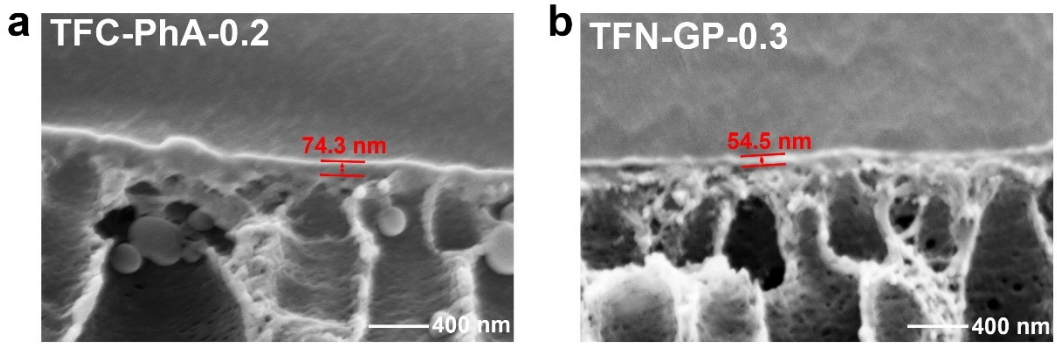

Figure S3. SEM cross-section images of (a) TFC-PhA-0.2 and (b) TFN-GP-0.3 composite membranes.

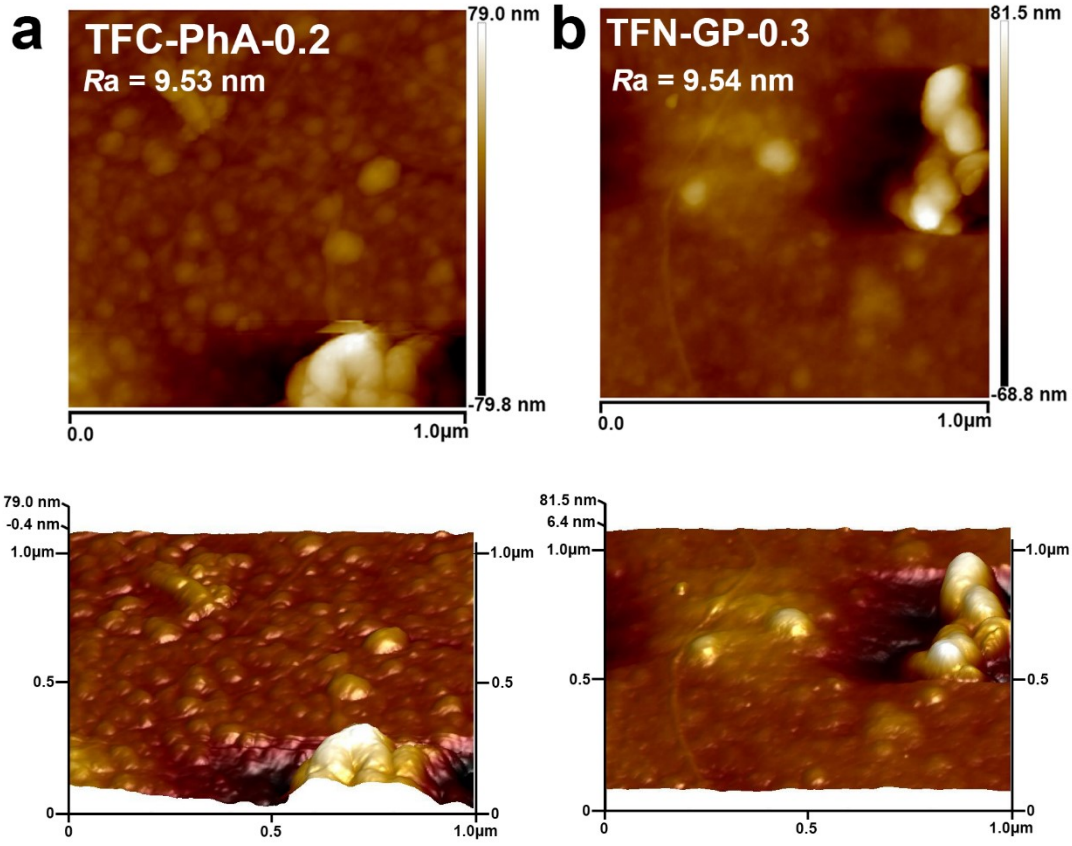

Figure S4. AFM surface images and the corresponding 3D surface morphology images of (a) TFC-PhA-0.2, (b) TFN-GP-0.3 membranes.

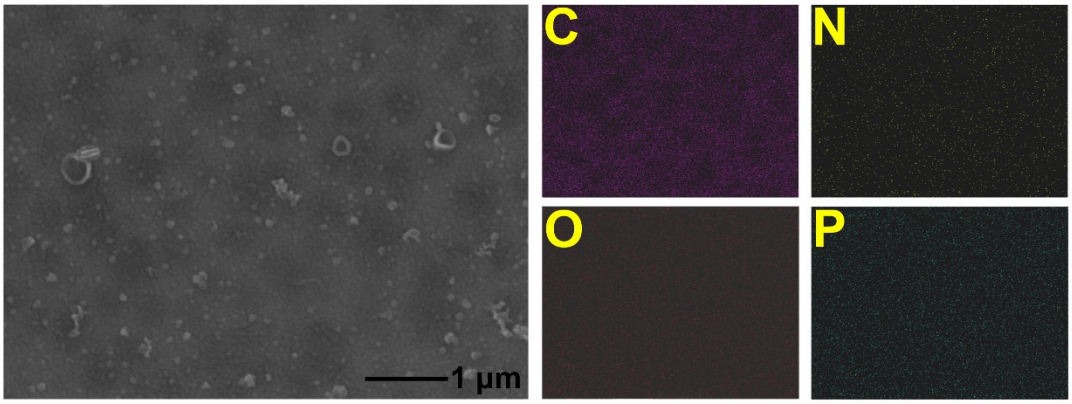

Figure S5. The surface EDS mappings of TFN-GP-0.2 membranes.

Table S1. Aqueous phase solution ratio of TFC and TFN composite nanofiltration membrane.

Membranes	Content of additive（wt%）	Content of PIP（wt%）	Content of CSA（wt%）	Content of TEA（wt%）
TFC	0	0.3	0.21	0.16
TFN-GO-0.2	0.2	0.3	0.21	0.16
TFC-PhA-0.2	0.2	0.3	0.21	0.16
TFN-GP1-0.2	0.2	0.3	0.21	0.16
TFN-GP5-0.2	0.2	0.3	0.21	0.16
TFN-GP10-0.2	0.2	0.3	0.21	0.16
TFN-GP15-0.2	0.2	0.3	0.21	0.16
TFN-GP10-0.05	0.05	0.3	0.21	0.16
TFN-GP10-0.1	0.10	0.3	0.21	0.16
TFN-GP10-0.15	0.15	0.3	0.21	0.16
TFN-GP10-0.2	0.20	0.3	0.21	0.16
TFN-GP10-0.25	0.25	0.3	0.21	0.16
TFN-GP10-0.3	0.30	0.3	0.21	0.16

Table S2. The roughness of TFC and TFN-GP composite membranes.

Membranes	Roughness	
	Ra (nm)	Rq (nm)
TFC	5.20	6.61
TFN-GO-0.2	5.33	6.77
TFC-PhA-0.2	9.53	16.0
TFN-GP-0.2	7.06	9.77
TFN-GP-0.3	9.54	16.3

Table S3. Elemental content by XPS of TFC and TFN composite membranes surface.

Membranes	C (%)	O (%)	N (%)	P (%)
TFC	70.32	17.43	12.25	/
TFN-GO-0.2	69.90	17.74	12.36	/
TFC-PhA-0.2	67.82	19.27	12.48	0.43
TFN-GP-0.2	68.31	18.69	12.64	0.36
TFN-GP-0.3	67.69	19.49	12.35	0.47

Table S4. Elemental content of TFN-GP10-0.2 composite membrane by XPS at 0, 20, 40 and 60nm sputtering depths.

Depth (nm)	C (%)	O (%)	N (%)	P (%)
0	68.31	18.68	12.64	0.37
20	72.88	14.53	12.23	0.36
40	75.22	12.48	11.97	0.33
60	79.59	11.10	9.01	0.30

Table S5. Comparison of separation performance in this study with various nanomaterials modified TFN nanofiltration membrane.

Additives	Operational condition	Flux（L m^{-2} h^{-1}）	Rejection rate（%）	Refs
UIO-66-NH_2	6 bar	44	91.2 ($MgSO_4$)	[4]
GO	6 bar	69.0	91.2 ($MgSO_4$)	[5]
GO	4 bar	62.5	96.6 (Na_2SO_4) 90.5 ($MgSO_4$)	[6]
GQD	2 bar	27.4	99.6 (Na_2SO_4) 99.5 ($MgSO_4$)	[7]
ZIF-8	4 bar	22.4	96.9 (Na_2SO_4) 92.9 ($MgSO_4$)	[8]
CTN	2.5 bar	23.8	95.0 (Na_2SO_4) 93.6 ($MgSO_4$)	[9]
CN/HNT	4 bar	63.6	94.5 (Na_2SO_4) 91.3 ($MgSO_4$)	[10]
O-MoS_2	3.5 bar	27.7	97.9 (Na_2SO_4) 96.5 ($MgSO_4$)	[11]
TA-MoS_2	4.5 bar	7.6	89.0 ($MgSO_4$)	[12]
HF-MoS_2	4 bar	21.5	97.75 ($MgSO_4$)	[13]
GP10	6.9 bar	48.9	98.3 (Na_2SO_4) 97.5 ($MgSO_4$)	This work

Reference

1. M. J. Abraham, T. Murtola, R. Schulz, S. Páll, J. C. Smith, B. Hess and E. Lindahl, *SoftwareX*, 2015, **1-2**, 19-25.
2. W. L. Jorgensen, J. Chandrasekhar, J. D. Madura, R. W. Impey and M. L. Klein, *Journal of Chemical Physics*, 1983, **79**, 926-935.
3. J. M. Wang, R. M. Wolf, J. W. Caldwell, P. A. Kollman and D. A. Case, *Journal of Computational Chemistry*, 2004, **25**, 1157-1174.
4. Y. Q. Gong, S. J. Gao, Y. Y. Tian, Y. Z. Zhu, W. X. Fang, Z. G. Wang and J. Jin, *Journal of Membrane Science*, 2020, **600**, 117874.
5. R. R. Hu, Y. J. He, C. M. Zhang, R. J. Zhang, J. Li and H. W. Zhu, *Journal of Materials Chemistry A*, 2017, **5**, 25632-25640.
6. W. Zhao, H. Y. Liu, N. Meng, M. P. Jian, H. T. Wang and X. W. Zhang, *Journal of Membrane Science*, 2018, **565**, 380-389.
7. Y. F. Li, X. D. You, Y. Li, J. Q. Yuan, J. L. Shen, R. N. Zhang, H. Wu, Y. L. Su and Z. Y. Jiang, *Journal of Materials Chemistry A*, 2020, **8**, 23930-23938.
8. J. Li, R. R. Liu, J. Y. Zhu, X. Li, S. S. Yuan, M. M. Tian, J. Wang, P. Luis, B. V. der Bruggen and J. Y. Lin, *Desalination*, 2021, **512**, 115125.
9. N. A. Khan, H. Wu, J. Q. Yuan, M. Y. Wu, P. F. Yang, M. Y. Long, A. U. Rahman, N. M. Ahmad, R. N. Zhang and Z. Y. Jiang, *Separation and Purification*

Technology, 2021, **274**, 119046.
10. Y. L. Liu, X. M. Wang, X. Q. Gao, J. F. Zheng, J. Wang, A. Volodin, Y. F. Xie, X. Huang, B. Van der Bruggen and J. Y. Zhu, *Journal of Membrane Science*, 2020, **596**, 117717.
11. S. S. Yang, Q. L. Jiang and K. S. Zhang, *Journal of Membrane Science*, 2020, **604**, 118052.
12. H. Zhang, X. Y. Gong, W. X. Li, X. H. Ma, C. Y. Tang and Z. L. Xu, *Journal of Membrane Science*, 2020, **616**, 118605.
13. X. P. Wang, Q. Xiao, C. Wu, P. Li and S. J. Xia, *Chemical Engineering Journal*, 2021, **416**, 129154.